Baseline concentrations, quantitative health risk assessment of polycyclic aromatic hydrocarbons (PAH), and the particle grain size of street dust in Warsaw, Poland

Sylwia Dytłow[1] (https://orcid.org/0000-0001-6968-6491), Jakub Karasiński[2] (https://orcid.org/0000-0003-3143-9131), Julio Cesar Torres-Elguera[3] (https://orcid.org/0000-0001-6598-5304)

[1]Institute of Geophysics Polish Academy of Sciences, Ks. Janusza 64, 01-452 Warsaw, Poland

[2]Faculty of Chemistry, Biological and Chemical Research Centre, University of Warsaw, Żwirki i Wigury 101, 02-089 Warsaw, Poland

[3]Department of Microbiology, Institute of Quality Sciences and Product Management, Krakow University of Economics, Sienkiewicza 4, 30-033 Krakow

Corresponding author details: Sylwia Dytłow skdytlow@igf.edu.pl

Keyword

Street dust; PAH; Carcinogenic health risk; Particle size distribution; Urban air pollution

Highlights

- Polycyclic aromatic hydrocarbons (PAH) were studied in 6 fractions of street dust.
- A fraction of grain diameter <0.2mm has the highest ∑PAH concentration.
- The highest cancerogenic risk was found for street dust of diameter <0.2 mm.
- Moderate and high health risks were obtained for PAH in street dust from Warsaw.

Abstract

Total concentrations, toxicity, and health risks of 16 polycyclic aromatic hydrocarbons (PAH) in street dust from Warsaw (Poland) in 6 granulometric fractions were investigated. Street dust was collected from 149 sampling points distributed among Area 1 (central districts, left bank of the Vistula River, mostly traffic-related pollution) and Area 2&3 (suburb area, mostly residential, right bank of the river). Street dust was investigated before ("all") and after separating into 5 size-dependent samples: (1–0.8 mm) "0.8", (0.8–0.6 mm) "0.6", (0.6–0.4 mm) "0.4", (0.4–0.2 mm) "0.2", and (below 0.2 mm) "<0.2". ΣPAH mean concentration was 3.21 mg/kg for Area 1 and 0.89 mg/kg for Area 2&3.

∑BaP_{TPE} values calculated collectively for Area 1&2&3 were observed to be 318.3, 83.5, 131.1, 81.4, 164.3, and 339.7 ng/g for "all", "0.6", "0.4", "0.2", and "<0.2", respectively. Significant differences in ∑BaP_{TPE} values were observed between fractions and specific areas. The cancer risk levels for children and adults, for all particulate size fractions, were comparable for dermal contact and by ingestion and ranged from 10^{-5} to 10^{-4}, whereas the cancer risk levels via inhalation always ranged from 10^{-10} to 10^{-8}. Therefore, inhalation of resuspended street dust is almost negligible compared to other pathways.

Environmental implication

Street dust pollution in cities is one of the most important issues in the world and it negatively affects the quality of the environment and people's health. This study contributed to filling the gap in knowledge about the characteristics of PAH contaminants in the subject of the grain size of street dust from Poland and assessing the potential health risks. Therefore, our work has provided new significant information on PAH pollution, methods of measuring PAH' content, and assessing the risk to human health, which may be useful to the scientific community, policymakers, and the general public.

1. Introduction

Environmental pollution in cities that concentrate a large number of people in a small area is one of the most important issues in the world and it negatively affects the quality of the environment and people's health (WHO, 2016). Street dust particles are considered to be one of the most important sources of fine aerosols in urban atmospheres and can become easily airborne through wind dispersion. Atmospheric aerosols, together with their chemical compounds from anthropogenic sources, tend to settle on the surfaces due to dry and/or wet deposition and are then incorporated into the street dust. United Nations (UN, 2019) reports that in 2018, 55% of the world's population lived in cities, and it is expected to reach 68% by 2050. The world's population increased from 6.1 billion in 2000 to 7.8 billion in 2020, of which the share of cities increased from ~47% to ~56% (Kaneda et al., 2015; UNDESA, 2018). This dense concentration causes an increasing amount of harmful pollutants to be produced in the urban environment, which exposes a large number of people to pollution resulting from anthropogenic activities in urbanized areas. Street dust is a heterogeneous composition

of soils and particles originating from natural and anthropogenic sources occurring on road surfaces by dry or wet deposition (Cao et al., 2017; Gunawardana et al., 2012; Haynes et al., 2020). Anthropogenic sources of different types of pollutants (e.g., heavy metals, polycyclic aromatic hydrocarbons (PAH)) in street dust originate from industrial and exhaust and non-exhaust traffic-related processes and low-stack emission andincluding fuel combustion, wear of tires, brake pads, road surface, body rust, leakage of brake and lubricating oil, automotive three-way catalytic abrasion and wear, and road paint (Kreider et al., 2010; Li et al., 2013; Logiewa et al., 2020; Pathak et al., 2013; Tanner et al., 2008; Yildirim and Tokalioğlu, 2016; Yang et al., 2010).

Polycyclic aromatic hydrocarbons (PAH) can originate from natural and anthropogenic sources. PAH are mainly produced and transferred into the environment due to incomplete combustion of fossil fuels and biomass, (Tobiszewski and Namiesnik, 2012; Tsibart and Gennadiev, 2013) but can also be produced during natural processes such as volcanic eruption (Kannan et al., 2005).

It is unambiguous that long-term exposure to air pollution provokes multiple health problems and diseases, such as atherosclerosis or respiratory endpoints health, including premature mortality. The results of the Aphekom project report (Aphekom, 2011) that living in close vicinity to busy roads is responsible for approximately 15–30% of all new cases of asthma in children and chronic obstructive pulmonary disease and coronary heart disease in adults older than 65 years of age.

There is a growing concern about the PAH pollution, which poses a significant environmental and health risk because of PAH' low aqueous solubility, semi-volatility, persistence, stability, and toxic properties (Larsen and Baker, 2003; Wang et al., 2015; Adeel et al., 2017). PAH can accumulate in the soil, street dust, and indoor dust and cause serious and harmful health effects for humans. The exposure to PAH poses health risks to the nervous system and different organs; it can contribute to the diseases of respiratory and circulatory systems and cancers (Sarigiannis et al., 2015). PAH pose a potential ecological risk and can damage human health through various absorption pathways such as direct ingestion, dermal contact, diet through the soil–food chain, inhalation, and oral intake (Franco et al., 2017; Lorenzi et al., 2011). Therefore, the study of PAH pollution of street dust is one of the most recent challenges in the field of protection of human health.

The main objectives of the present study were as follows: (1) to evaluate the total PAH concentration levels content in the street dust collected from different land use patterns; (2) to investigate the particle size effect on the distribution of the PAH concentrations; (3) to characterize the spatial distribution of the total concentrations of street dust for the finest fraction of less than 200μm in diameter; and (4) to assess the human health risks posed by PAH for children and adults via ingestion, inhalation, and dermal contact and according to different particle size.

2. Methods

2.1. Study area

The sampling campaigns were carried out in the administrative area of the capital city of Poland - Warsaw. Warsaw (52°13′48″N 21°00′40″E) is situated in the Mazovian region along the Vistula River. The city straddles the Vistula River. It is located in the heartland of the Masovian Plain, and its average elevation is 100 m (330 ft) above sea level. The area of the Warsaw agglomeration is 517.24 km^2. The city is characterized by a dense network of streets and railways, but relatively low industrialization, except from three combined heat and power plants: Siekierki, Kawęczyn, and Żerań. The population is ~1.8 million, but many estimates suggest that the number of residents may be closer to 2.4 million (GUS, 2023).

2.2. Description of the sampling location

The street dust sampling campaign was carried out according to a pre-identified plan. The sampling sites were located in different functional areas (industrial, traffic, commercial, residential, and green areas) in the administrative area of Warsaw. Street dust was sampled from the following areas: the central district of the city (Area 1) and peripheral districts - Rembertów (Area 2)/Wawer (Area 3). A number of 100 samples were collected from Area 1 on the left bank of the Vistula River and 49 samples from Area 2 and Area 3 on the right bank of the Vistula River. The land use of Area 1 is mostly the commercial area and city center with high road density, population density, and vehicle flux. Area 2 is dominated by large green areas and low population density. The sampling sites were described in terms of traffic intensity, i.e., the number of vehicles passing through it in both directions in 24 hours (WBR, 2023). In this way, each location was assigned to one of the following categories:

low (1) (<5000 veh./day), medium (5000–10000 veh./day), high (10000–20000 veh./day), and very high (>20000 veh./day) traffic intensity.

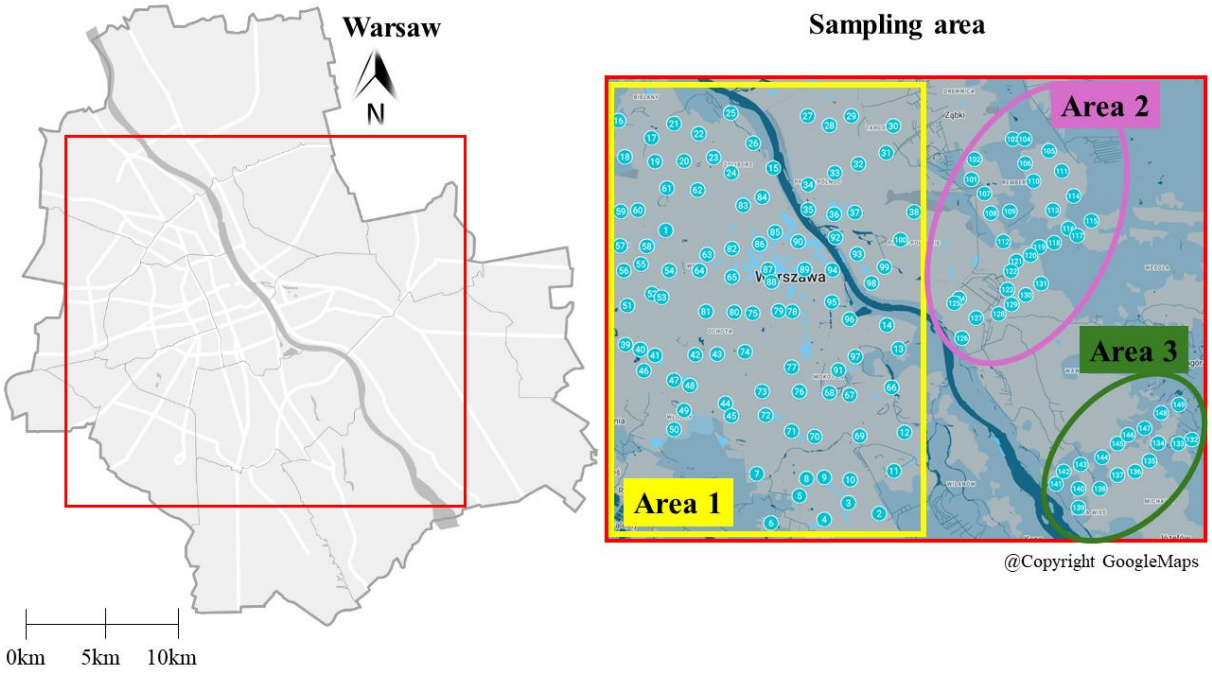

Figure 1. Locations of the 149 sampling sites in Warsaw.

2.3. Sample preparation of street dust

Street dust was collected from 149 sampling sites in the Warsaw urban area (Fig. 1) and geolocalized using a handheld GPS device. The samples were collected from ~1 m^2 area of the road surfaces using a clean plastic vacuum cleaner or by sweeping with a brush into a plastic dustpan. All collected samples were a composite of subsamples collected within a 5-m radius. The sampling campaigns were performed after seven no rainy days to ensure street dust accumulations become relatively not influenced by the runoff. The road area covered by sampling included the zone between the curb and the road axis, with particular emphasis on the zone along the curb. This procedure is necessary because most of the dust accumulates along the curb (Deletic and Orr, 2005; Dytłow et al., 2019). The sampling points were selected to represent different land-use categories, traffic intensity, and population density. Additionally, the sampling sites were selected specifically to represent motor traffic of significant traffic density on a transit road with modern infrastructure and to represent the areas polluted by low-stack emissions.

2.4. Granulometric segregation and sample selection for chemical analysis

The sampling was collected from September to November 2023. For each site, ~500 g of dust was collected, placed into coded self-sealing polyethylene bags, and transported to the laboratory. After being transferred to the laboratory, the samples were air-dried at room temperature (approximately 25 °C) and relative humidity of 20% for 7 days before undergoing further analysis.

The samples were initially sieved through a 1 mm mesh to remove waste, leaves, roots, and small stones. These samples were labeled “all” and a sample was taken for further determination of PAH concentration. The remaining part of the sample was separated using sieves with different mesh sizes. The granulometric analysis was performed using a laboratory shaker LPzE-2e (MULTISERW-Morek, Poland) with a set of sieves of the following mesh sizes: 1 mm, 0.8 mm, 0.6 mm, 0.4 mm, and 0.2 mm. Therefore, the following particle size fractions were obtained: diameter between 1 and 0.8 mm (fraction “all”), between 0.8 and 0.6 mm (fraction “0.8”), between 0.6 and 0.4 mm (fraction “0.6”), between 0.6 and 0.4 mm (fraction “0.4”), between 0.4 and 0.2 mm (fraction “0.2”), and less than 0.2 mm (fraction “<0.2”).

As a result of applying the above-described procedure, 6 samples were obtained for each of the 149 sampling sites, giving a total number of 894 samples. The 169 samples representing all granulometric fractions, different land use, and located in every studied area (Area 1, Area 2, and Area 3 (Fig. 1)) were selected for further chemicalanalyses.

2.5. Data analysis

The data was processed using Microsoft Excel 2019 for statistical calculations and table preparation. The Origin2019 software (OriginLab Corporation, US) was utilized to draw all presented graphs and the spatial distribution map. The Delauney triangulation scheme implemented into Origin2019 software was applied to interpolate the data between sampling sites on the spatial distribution map. Figure 2 was made using MS Excel 2021.

2.6. Chemical analysis

2.6.1. Sample preparation.

Before proceeding to the quantitative analysis of PAH, it was necessary to extract these compounds from street dust samples. Analyses were carried out both without dividing the samples into fractions and after separating the sample from a given site into individual fractions. Initially, acetonitrile (ACN)

extraction, as described by Puy-Alquiza et al. (2016), was used. However, this procedure has been a subject to some modifications. Based on the analysis of reference material (LGC6188), the influence of extraction time on its efficiency was checked. Several preconcentration factors were investigated to obtain compromise conditions between the signal intensity and the negative influences of matrix effects (and thus obtain the most favorable signal-to-noise ratio). Finally, the following procedure was used: Approximately 5g of the homogenized sample was weighed. 25 ml of ACN was added. The sample was mechanically shaken for approximately 3 minutes, and then, ultrasonic-assisted extraction was performed. Extraction was carried out in a closed system at a temperature of 30 ^{o}C for 2 hours. The temperature of 30^{o}C is a compromise value that allows for achieving sufficient efficiency without evaporating the most volatile PAH (despite the closed system). The extract was then separated from the solid residue by centrifugation (Eppendorf 5804R) at 4200 rpm at room temperature. The last step was to evaporate the samples to dryness at 30^{o}C in the SpeedVac (Eppendorf Concentrator Plus) system. Then, 500 μL of ACN was introduced into the vessel and left for approximately 10 minutes. Then, it was shaken mechanically for about 2 minutes and transferred to a chromatographic vail.

2.6.2. Measurement procedure

Total PAH content was calculated as a sum of 16 compounds present in the standard (Supelco, CRM47940 PAH Calibration Mix). The chemical compounds whose concentrations were monitored are presented in detail in Table S1 (see Supplementary materials). To investigate concentrations of individual PAH, a method combining high-performance liquid chromatography (HPLC, Agilent 1290) with a series-connected spectrophotometric detector (Agilent G4212B 1260 Diode Array Detector) and a mass spectrometer (Agilent 6460) with a triple quadrupole mass analyzer (QQQ). QQQ was fitted with the APCI source (atmospheric pressure chemical ionization) operated in the positive ion mode. Initially, the instrument was operated in scan mode, and after determining m/z characteristics for each PAH, the registration mode was changed to Single Ion Monitoring to improve sensitivity. A chromatographic column designed for this type of separatiosn (Phenomenex, Kinetex 3.5 μm PAH, 100*2.1 mm) was used to separate 16 PAH present in the standard (Supelco, CRM47940 PAH Calibration Mix). Gradient elution was used: 0.1% formic acid (FA, Supelco LC-MS LiChropur) in water (Supelco LiChrosolv LC-MS Grade water) was used as a mobile phase with a lower elution

strength, and 0.1% FA in ACN (Supelco LiChrosolv hypergrade for LC-MS) as a phase with a higher elution strength. Parameters of chromatographic separation and detection are shown in Table S1. When developing the method, five different ways of signal acquisitions were checked: 356 nm without reference, 541 nm without reference, 370 nm without reference, 254 nm with reference at 400 nm, and 292 nm with reference at 400 nm. The method giving the best sensitivity of the determinations was selected: 254 nm with reference at 400 nm (Mansouri et al., 2020). Then, the results obtained for both detectors (MS and DAD) were compared. Additionally, based on the obtained mass spectra, the order of elution of individual PAH was confirmed. Due to the high consistency of the results between both detectors, only UV detection was used after the method development was completed. All presented results were obtained by UV detection. Identification of individual PAH was based on a comparison of the retention times of a given compound in the standard and sample. The extraction efficiency and validity of the proposed measurement procedure were confirmed by analyzing matrix certified reference materials (LGC6188, NIST2768). The results obtained for reference materials were also used to estimate the standard uncertainty of PAH measurement.

2.7. Carcinogenic PAH (CPAH) determination

CPAH are determined by the sum of the concentration of carcinogenic PAH (CPAH = BaA + Chry + BbF + BkF + BaP + DBA + IP) listed by the International Agency for Research on Cancer (IARC, 1987) and expressed as a percentage to other PAH in this study. CPAH were calculated for samples "all" and for each granulometric fraction.

2.8. Benzo [a] Pyrene equivalent (BaP) toxicity

The quantities of toxicity potential were assessed by calculation of benzo(a)pyrene total equivalency (BaP_{TPE}) for PAH. BaP_{TPE} was obtained using BaP toxicology equivalency factors (TEFs). B[a]P TPE is the sum of estimated cancer potency relative to BaP for all carcinogenic PAH, which was calculated by multiplying the concentration of each carcinogenic PAH in the same sample by its BaP_{TEFs} (Nisbet and LaGoy, 1992; Soltani et al., 2015). The TEF estimates for Nap, Acy, Ace, Flu, Phen, Anth, Flan, Pyr, BaA, Chry, BbF, BkF, BaP, DBA, BghiP, and IP are 0.001, 0.001, 0.001, 0.001, 0.001, 0.01, 0.001, 0.001, 0.1, 0.01, 0.1, 0.1, 1, 1, 0.01, and 0.1, respectively. BaP toxicology equivalency factors (TEFs) were used to evaluate BaP_{TPE} for PAH using the following equation:

$$BaP_{TPEi}\ (ng/g) = C_i \times TEF_i,$$

where C_i is the specific concentration of PAH.

$$\sum BaP_{TPE}\ (collective) = \sum^{i} BaP_{TEFi},$$

in which BaP_{TPE} (collective) is the BaP equivalent concentration obtained by summing the masses of individual compounds (C_i), each weighted by its relative cancer potency, TEF_i (Ma and Harrad, 2015).

2.9. Potential health risk assessment

In this study, the potential non-carcinogenic and carcinogenic health risks of both groups of Warsaw residents, adults and children, were quantified according to the models developed by the United States Environmental Protection Agency (USEPA, 2011; USEPA, 2014). It was assumed that PAH unintentionally penetrate the body through oral, inhalation, and dermal routes (exposure paths). Another assumption proposed by USEPA was the duration of life during which residents are exposed to PAH. In the case of adults, USEPA assumes that it would be 70 years, and in the case of children – 6 years. The environmental exposure was estimated based on the average dose, which determines the amount of harmful substance taken by the studied population per day and per 1 kg of body weight.

The incremental lifetime cancer risk (ILCR) of a chemical substance received through each of the main three pathways, ingestion ($ILCR_{ing}$), inhalation ($ILCR_{inh}$), and dermal contact ($ILCR_{derm}$) was calculated according to the following equations (USEPA, 2011):

$$ILCR\ ingestion = \frac{CS \times IR\ ingestion \times EF \times ED \times \left((CSF\ ingestion) \times \sqrt[3]{\frac{BW}{70}}\right)}{BW \times AT \times 10^{6}},$$

$$ILCR\ inhalation = \frac{CS \times IR\ inhalation \times EF \times ED\ \times \left((CSF\ inhalation) \times \sqrt[3]{\frac{BW}{70}}\right)}{BW \times AT \times PEF},$$

$$ILCR\ dermal = \frac{CS \times SA \times AF \times ABS \times EF \times ED \times \left((CSF\ dermal\ contact) \times \sqrt[3]{\frac{BW}{70}}\right)}{BW \times AT \times 10^{6}},$$

240

241 Carcinogenic risk (CR)= ILCR ingestion + ILCR inhalation + ILCR dermal contact,

242

243 where *CS* is the PAH concentration of the dust sample (mg/kg) calculated as the sum of converted
244 PAH concentrations based on TEF values as proposed by Nisbet and LaGoy (1992). *CSF* stands for
245 the carcinogenic slope factor, which is measured by the following unit: (mg/kg)/day. The CSFs of BaP
246 values, as reported by the US EPA, are 25, 7.3, and 3.85 (mg kg/day) for the selected paths in this
247 study, which are dermal contact, oral ingestion, and inhalation, respectively (Chen et al., 2013; Peng et
248 al., 2011). $IR_{ingestion}$ is the dust intake rate (in mg/day); $IR_{inhalation}$ is the inhalation rate (in m^3/day);
249 *EF* is the exposure frequency (in day/year); *ED* is the exposure duration (in years); *PEF* is the particle
250 emission factor (in m^3/kg); *SA* is the exposed skin area (in cm^2/day); *SAF* is the skin adherence factor
251 (in mg/cm^2); *ABS* is the dermal absorption factor (chemical-specific, unitless); *BW* is the body weight
252 (in kg); and *AT* is the averaging time (in days). The parameters referred to the models' values for
253 children (1–6 years old) and adults (7–31 years old) are based on the Risk Assessment Guidance of
254 USEPA and listed in Table S2 (see Supplementary material). Other parameters used for ILCR
255 calculations are also described in Table S2.

256 **3. Result and discussion**

257 **3.1. Total PAH concentrations on different particle sizes**

258 The total PAH contents in individual fractions are shown in Table 1. It is the most visible that the
259 highest concentration of these compounds was found in the fraction with the smallest grain diameter.
260 For most samples, the total PAH content in the "<0.2" mm fraction was the highest and often
261 exceeded the total content in the sample without division into fractions. A typical course of PAH
262 concentration variability depending on the fraction is shown in the form of a whisker plot in Figure 2.
263 The dependence is shown here separately for samples from Area 1 and Area 2&3. Samples without
264 fractionation are characterized by relatively high levels of PAH. Then, for fractions "0.8" mm, "0.6"
265 mm, and "0.4" mm, PAH content drops significantly. For fraction "0.2", it increases noticeably to
266 reach a maximum for fraction "<0.2" mm. Despite this common characteristic, a comparison of

dependencies for Area 1 and Area 2&3 reveals several significant differences in average total PAH concentration depending on the fraction. What differs the most between these two dependencies is the level of PAH in the “0.6” mm and “0.2” mm fractions. In the case of Area 1 samples, fraction “0.6” mm has a higher average level of PAH compared to the corresponding fractions “0.4” mm and “0.8” mm. In the case of samples from Area 2&3, the lowest average level of these compounds was found just in fraction “0.6” mm. It should also be noted that the average PAH level in the “0.2” mm fraction is much higher in Area 1 compared to Area 2&3. The general observation is that in the case of Area 2&3, PAH are concentrated almost exclusively in the “<0.2” mm fraction, while in the case of Area 1, this distribution is more even.

Comparing our total content results with those presented by other researchers, we note general consistency of results. In our work, the average content of PAH content in the sample without division into fractions was 2.6 mg/kg, reaching a maximum of 7.0 mg/kg. Other researchers presented similar average PAH contents, such as from 1.3 mg/kg to 8.0 mg/kg (Puy-Alquiza et al., 2016), or from 0.84 mg/kg to 12.3 mg/kg with an average value of 4.8 mg/kg (Wang et al., 2011). Similar levels of total PAH content were also reported by others (Franco et al., 2017; Gope et al., 2018; Wang et al., 2015). Despite efforts, we did not find many publications with information on the total content of PAH divided into fractions. However, we found information confirming that PAH are mainly found in fractions with low granulation. For example, Dong (Dong and Lee, 2009) observed the highest PAH concentrations in the <0.063 mm and 0.063 - 0.180 mm fractions, which approximately corresponds to the <0.2 mm fraction from our work. Similarly, Murakami (Murakami et al., 2005), who investigated the PAH content in road dust of two districts of Tokyo, presented results showing that the highest levels of PAH are found in fractions with low granulation, for example, 0.063 mm. Ha (Ha et al., 2012), who investigated PAH levels in Masan, Korea, divided the sample into fractions below 0.063mm, 0.063mm - 0.125mm, 0.125mm - 0.300mm, and 0.300 - 0.600mm and fractions with larger granulation. Ha et al. (2012) showed values of the total PAH content in samples from areas with heavy road traffic that were very similar to ours. These values ranged from 0.45 to 14.0 mg/kg, depending on the fraction. For most of the samples, Ha presented that the highest total PAH content is for light fractions, i.e., below 0.300 mm.

Fraction (Area 1&2&3)	Total PAH concentration in different particle sizes fraction [mg/kg]					
	"<0.2"	"0.2"	"0.4"	"0.6"	"0.8"	"all"
n (number of samples)	51	22	16	23	33	18
Min	1.0	0.1	nd*	nd*	nd*	0.1
Max	11.1	10.0	2.2	10.8	3.5	7.0
Average	3.4	1.9	0.7	1.4	0.9	2.6
SD	2.1	2.5	0.8	2.3	1.0	2.3

* nd = not detected

Table 1. Total PAH concentration in different particle sizes fraction from Area 1&2&3.

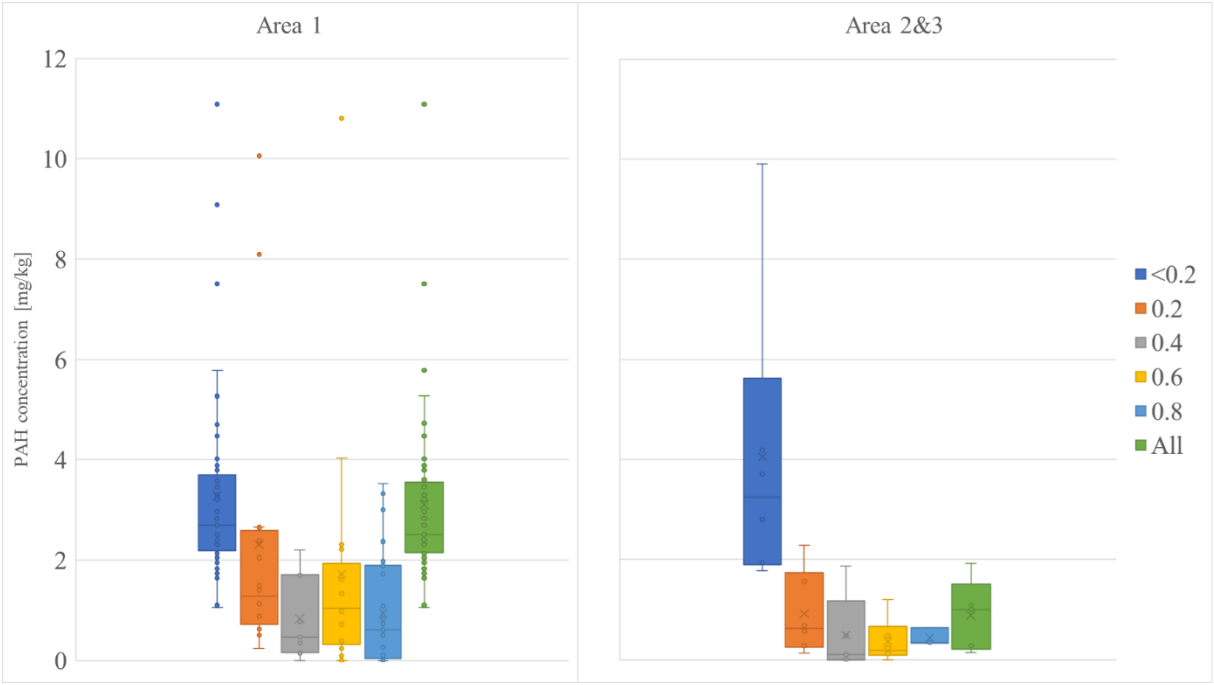

Figure 2. Whisker plots for total PAH concentration for each fraction divided into Area 1 and Area 2 & 3. Whiskers contain the maximum value, average value, and minimum value. The black horizontal lines represent the averages. The bottom and top of the boxes represent the first and the third quartiles. Single points are outliers. All values are given in mg/kg.

3.2. Individual PAH analysis

303 Table 2 shows the average content of 16 analyzed PAH (in samples without separation into fractions),
304 as well as the minimum and maximum values. The average total PAH content in samples from central
305 districts (Area 1) and peripheral districts (Area 2&3) is also presented.

Name	**Individual PAH concentrations in "all" fraction Area 1&2&3 [mg/kg]**		
	Min	**Max**	**Average**
Naphthalene	nd*	nd*	nd*
Acenaphthylene	nd*	1.34	0.17
Acenaphthene	nd*	1.82	0.48
Fluorene	nd*	0.20	0.02
Phenanthrene	nd*	0.97	0.22
Anthracene	nd*	0.75	0.08
Fluoranthene	nd*	1.55	0.34
Pyrene	0.07	1.40	0.33
Benz(a)anthracene	nd*	0.61	0.12
Chrysene	0.03*	0.62	0.16
Benzo(b)fluoranthene	0.03*	0.38	0.12
Benzo(k)fluoranthene	Nd	0.26	0.06
Benzo(a)pyrene	Nd	0.90	0.26
Dibenz(a,h)anthracene	Nd	0.10	0.02
Benzo(ghi)perylene	Nd	0.26	0.10
Indeno(1,2,3-C,D)pyrene	Nd	0.22	0.09
Average $\sum PAH_{16}$ Area 1&2&3 All	2.05		
Average $\sum PAH_{16}$ Area 1 All	3.21		
Average $\sum PAH_{16}$ Area 2&3 All	0.89		

306 *nd = not detected

307 Table 2. Individual PAH concentration in “all” fraction from Area 1&2&3 and average $\sum PAH_{16}$ for
308 Area 1&2&3, Area 1, and Area 2&3.
309 Analyzing the data presented in Table 2, it should be noted that naphthalene was not detected in any of
310 the samples. The main PAH present in the samples include Acenaphthene, Fluoranthene, and Pyrene.
311 This observation is consistent with data published by Dong and Lee (2009) and Puy-Alquiza et al.
312 (2016). Puy-Alquiza indicates Fluoranthene and Pyrene as the two PAH with the highest
313 concentration. Dong and Lee (2009) indicates Acenaphthene, Fluoranthene, and Pyrene as the three
314 most concentrated PAH. In our work, we also point out that these three compounds contribute the
315 most to the total PAH content in the investigated samples. The compounds with the least importance
316 are Fluorene, Anthracene, Benzo(k)fluoranthene, and Dibenz(a,h)anthracene. Acenaphthene has the
317 highest variability in terms of content (from nd to 1.82 mg/kg). Regarding the differences between
318 samples from Area 1 and Area 2&3, for all samples, the mean content of each PAH was higher for
319 samples from Area 1. Additionally, Acenaphthylene and Acenaphthene, compounds that were
320 dominant in samples from Area 1, were not detected at all in samples from Area 2&3. Large
321 differences between Area 1 and Area 2&3 also occur in the case of Fluoranthene and Benzo[a]pyrene.
322 Ultimately, the average total PAH content in samples from Area 1 is almost four times higher than in
323 samples from Area 2&3.
324 **3.3. Uncertainty estimation**
325 Error propagation was used to estimate the uncertainty of the total PAH concentration results, which
326 are the sum of the concentrations of 16 individual chemical compounds monitored during analysis
327 (listed in Table 2). To estimate the measurement uncertainty of each of the 16 individual PAH,
328 repeated analyses of two matrix reference materials (LGC6188, NIST2768) with certified PAH
329 content were performed. To correctly estimate the uncertainty of concentration results, the two most
330 important uncertainty components were taken into account: one related to the difference between the
331 measured and expected value (result trueness, estimated from recovery tests) and the other related to
332 the repeatability of the result (precision of repeated measurements). It should be emphasized that since
333 matrix reference materials (CRM) were used, it was possible to calculate the recovery for each
334 individual PAH. CRMs were prepared and measured in a manner identical to that of the analytical

samples. Doing so allows us to take into account the uncertainty associated with sample preparation as well as the uncertainty associated with the calibration and measurement itself. To our knowledge, this is the best available way to estimate the trueness of the results for this type of measurement. In each of the five measurement sessions, the LGC6188 reference material was prepared from a new aliquot, so it was subjected to the full sample preparation procedure. The NIST material was prepared only in two sessions due to limited availability. Then, in each session, a given analytical sample deriving from a current aliquot of the material was analyzed five times. Based on the obtained results, recoveries and repeatability were calculated for each of the individual PAH. Using the error propagation method (where the components were recovery describing the trueness of the result and repeatability describing precision), the standard uncertainty for each PAH was calculated, and finally, the standard uncertainty for determining the total content. Standard uncertainties for individual PAH ranged from 5% to 17%. The standard uncertainty of determining the total PAH content was estimated at the level of 14%. We emphasize that to estimate the uncertainty for the total PAH content, we used propagation of error expressed in concentration units, not in percentages. Using the uncertainty for individual PAH expressed in % to propagate the error for the total content would lead to an overestimation of the measurement uncertainty.

3.4. Toxicity in terms of Carcinogenic PAH (CPAH)

The percentage composition of carcinogenic PAHPAH (CPAHPAH = BaA + Chry + BbF + BkF + BaP + DBA + IP), listed by the International Agency for Research on Cancer (IARC, 1987) to other PAH has been illustrated in Figure 3. The results for all sampling sites were analyzed both collectively (Area 1&2&3) and after division into Area 1 and Area 2&3. This approach is justified due to the different characteristics of these areas in terms of land use and dominant emission sources. Area 1 is located on the left bank of the Vistula River and includes central districts with heavy vehicle traffic and a centralized building heating system. In turn, Area 2&3, located on the right bank of the Vistula River, is dominated by residential areas, larger green areas than those in Area 1, and more diversified intensity of vehicle traffic (ranging from local roads with <2000 vehicles/day and medium/heavy traffic roads with >10000 vehicles/day). For Areas 1&2&3, the average CPAH contributions for fractions “all”, “0.8”, “0.6”, “0.4”, “0.2”, and “<0.2” were found to be 31, 21, 34.5, 32, 34, and 24%,

respectively. CPAH were also calculated separately for Area 1 and Area 2&3 to capture potential differences in CPAH across all three investigated Areas. The CPAH values obtained for Area 1 are similar to the results obtained for the collective calculation for Area 1&2&3. Percentages of CPAH for Area 1 are 28.5, 19, 29.5, 33, 32, 22.5% for fractions “all”, “0.8”, “0.6”, “0.4”, “0.2”, “<0.2”, respectively. CPAH values for Area 2&3 were higher in all fractions and for "“all”" samples compared to CPAH values for Area 1 and Area 1&2&3. The largest difference was recorded for the "“0.8”" fraction, for which CPAH for Area 1 were 19% and for Area 2&3 52.5%. The CPAH values for the remaining grain size ranges from Area 2&3 are 37, 52.5, 30, 41, and 38.5% for “all”, “0.6”, “0.4”, “0.2”, and “<0.2”, respectively.

The results of CPAH for this study are in general accordance with other reported PAHresults of CPAH. Yusuf et al. (2022) reported that overall mean CPAH contribution for Ibadan (Nigeria) was 50%. Gope et al. (2018) recorded a mean CPAH contribution of 43% for street dust from Asansol (India). The other study for street dust from India (city of Guwahati) reported (Hussain et al., 2015) that CPAH accounted for 33%, which is about 3 times lower than CPAH for Kurukshetra (India) (Kamal et al., 2015). CPAH content calculated for Areas 1&2&3 ranged from 0 to 3.96 mg/kg with an average of 0.56 mg/kg. Even assuming that street dust does not enter the body directly through ingestion (as is the case with CPAH contained in food), the average CPAH amount exceeds significantly the 0.137 mg/kg limit (Department of Ecology, State of Washington, 2007) for clean-up established by the Department of Ecology, State of Washington (2007). Taking into account the above recommendation, preventive cleaning is required to counteract any possible adverse health effects resulting from PAH contamination contained in street dust from Warsaw.

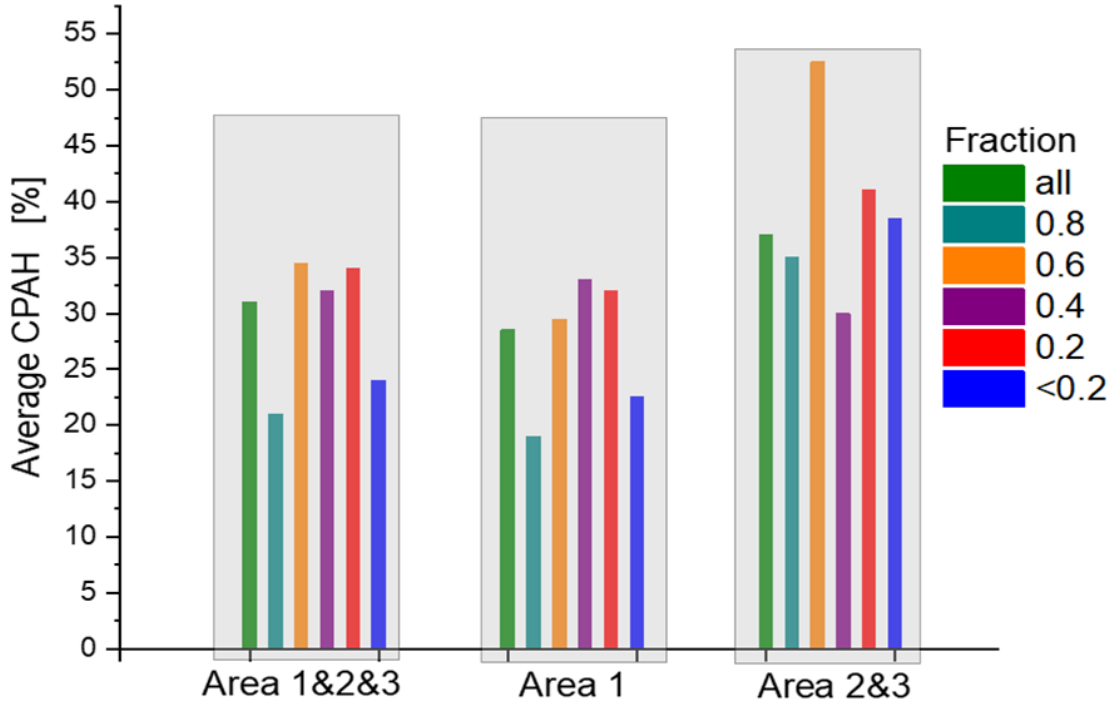

Figure 3. Average percentage contribution of carcinogenic PAH (CPAH %) for fractions “all”, “0.8”, “0.6”, “0.4”, “0.2”, and “<0.2” and Areas 1&2&3, Area 1, and Area 2&3.

3.5. Toxicity in terms of BaP toxicity equivalent

$\sum BaP_{TPE}$ and TEFs of each of the PAH were used to evaluate the toxic and carcinogenic potency of the street. Figure 4 and Table S3 summarize the results of the BaP toxic equivalent concentrations of street dust for all granulometric fractions of Areas 1&2&3 and separately for Area 1 and Area 2&3. $\sum BaP_{TPE}$ values calculated for all studies areas (collectively for Areas 1&2&3) were observed to be 318.3, 83.5, 131.1, 81.4, 164.3, and 339.7 ng/g for “all”, “0.6”, “0.4”, “0.2” and “<0.2”, respectively. Significant differences in $\sum BaP_{TPE}$ values were observed between fractions. The ""“<0.2”"" fraction had the highest values and were 339.7, 318.9, and 531.6 for Areas 1&2&3, Area 1, and Area 2&3, respectively. The lowest average $\sum BaP_{TPE}$ values for Area 1&2&3 (81.4), Area 1 (64.1), and Area 2&3 (40.5) were observed in coarser fractions “0.4”, “0.8”, and “0.6”, respectively. The largest differences between Area 1 and Area 2&3, in terms of the distribution of the parameter depending on the fraction, were recorded in the fractions ""“0.8”"" and ""“0.6”"". For the “0.6” samples, in the case of Area 1, $\sum BaP_{TPE}$ was almost 4 times higher than for Area 2&3, reaching a value of 157 ng/g for Area

1 and 40.5 ng/g for Area 2&3. In the case of fraction "0.8", the opposite pattern was observed. $\sum BaP_{TPE}$ was more than 3 times higher for Area 2&3 than for Area 1 and equaled 64.1 ng/g for Area 1 and 214.6 ng/g for Area 2&3.

Generally, the $\sum BaP_{TPE}$ values for Warsaw street dust are lower than in other studies. The$\sum$ BaP_{TPE} values for street dust from industrial areas and urban areas from Ulsan (Korea) (Dong and Lee, 2009) ranged from 0.93μg/g to 16.74 μg/g and from 4.37 μg/g to 68.84 μg/g, respectively. At different sampling sites in Asansol (India), Gope et al. (2018) reported that for the street from Asansol (India), BaP_{TPE} concentrations varied between 294 ng/g and 1421 ng/g, with a mean value of 661 ± 280 ng/g.

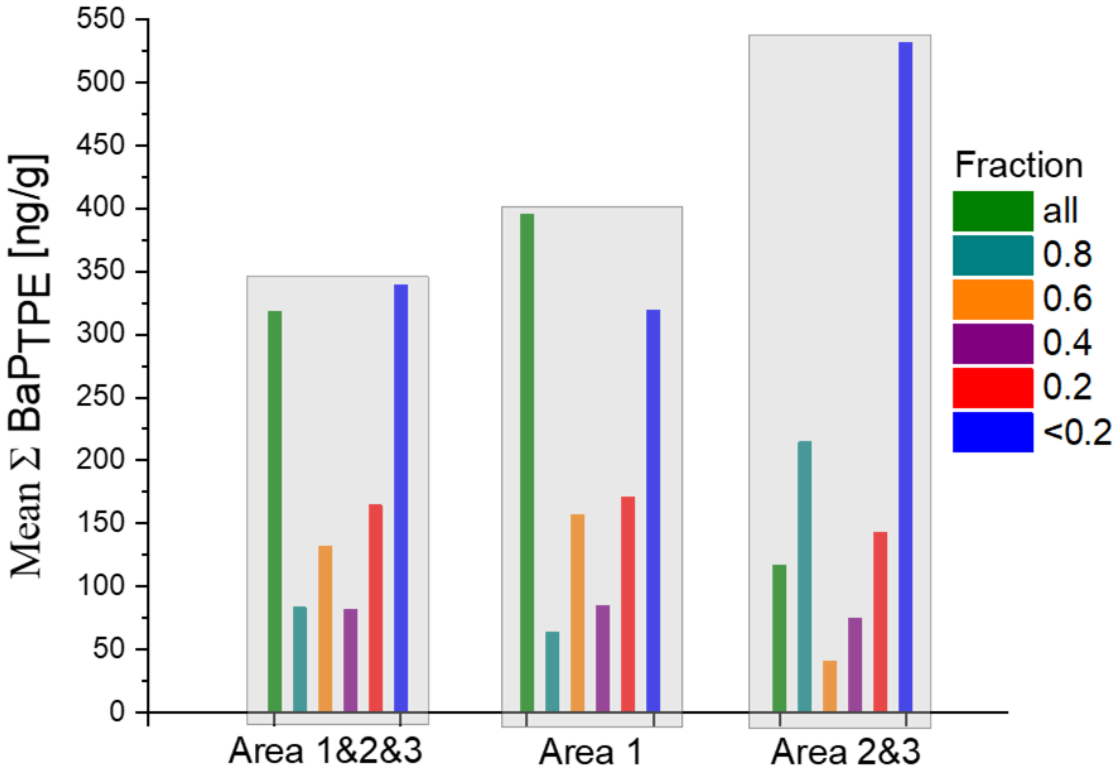

Figure 4. Mean summary contribution of benzo(a)pyrene total equivalency ($\sum BaP_{TPE}$) for PAH. $\sum BaP_{TPE}$ was calculated for fractions "all", "0.8", "0.6", "0.4", "0.2", and "<0.2". $\sum BaP_{TPE}$ was calculated collectively for Areas 1&2&3 and separately for Area 1 and Area 2&3.

3.6. Health risk assessment

The present study is the first one that evaluated the potential cancer risk arising from human exposure to PAH in street dust for six different granulometric fractions and different functional areas. Based on the Toxic Equivalence Factor (TEF), a probabilistic risk assessment framework, was used to estimate age-specific potential cancer risks arising from exposure to cancerogenic PAH entering the human body via different pathways, i.e., inhalation, ingestion, and dermal contact. Based on the daily exposure level, the ILCRs were estimated, and the results are listed in Figure 5 (a-h) and Table S4. For all studied Areas, the highest ILCRs for adults and children for every pathway type were obtained for Fraction "<0.2". The mean cancer risk levels via dermal contact and ingestion pathway ranged from 10^{-5} to 10^{-4} in all granulometric fractions, while the mean cancer risk via inhalation was 10^{-10} to 10^{-8}, which implies $ILCR_{inhalation}$ was from three to six magnitudes lower than that through ingestion and dermal contact. This observation implies that inhalation of resuspended street dust particles through the mouth and nose was of less importance when compared with the other routes. This finding is in agreement with other studies of street dust from Asaluyeh County and Qom metropolis (Iran) (Abbasi and Keshavarzi, 2019; Davoudi et al., 2021), Punjab province (Pakistan) (Kamal et al., 2014), Novi Sad city (Serbia) (Skrbic et al., 2019) and Guangzhou (China) (Wang et al., 2011).

The total carcinogenic risk (CR) was calculated for three exposure pathways as a sum of the three individual risks. USEPA (2011) states the acceptable risk range of carcinogens is 10^{-6}–10^{-4} (USEPA 2011). Risks lower than 10^{-6} do not need further intervention, whereas risks higher than 10^{-4} require actions to minimize exposure and subsequent harm (USEPA, 2011). The maximum and minimum mean values of CR for children were obtained for Area 2&3 and ranged from 7.13×10^{-5} for fraction "0.6" to 9.35×10^{-4} for fraction "<0.2" (Fig. 5h). The same pattern was observed for the mean CRs calculated for adults. The lowest mean CR was also observed for fraction "0.6" (1.07×10^{-4}) from Area 2&3 and the highest mean CR similar to the calculation for children was observed for fraction "<0.2" (1.41×10^{-3}) from Area 2&3 (Fig. 5g). For both adults and children, for all investigated Areas and granulometric fractions, the CR is of the order of 10^{-4} and 10^{-3}. Only in one case, i.e., for CR for Area 2&3 for children and only for the ""0.6"" fraction, CR is of the order of 10^{-5}. This showed that the risk arising from exposure to PAH in street dust is significant for Warsaw residents and it is

recommended to take steps to reduce exposure to street dust. The ILCRs for the finest fraction "“<0.2”" were two to five times significantly higher compared to coarser fractions. All CRs for the "“<0.2”" fraction represent a high (10^{-4}) or very high (10^{-3}) carcinogenic risk. Small particles enter the human body more easily, and due to their small size, they can even penetrate the human bloodstream, which, in addition to the concentration of PAH, increases their harmfulness to health.

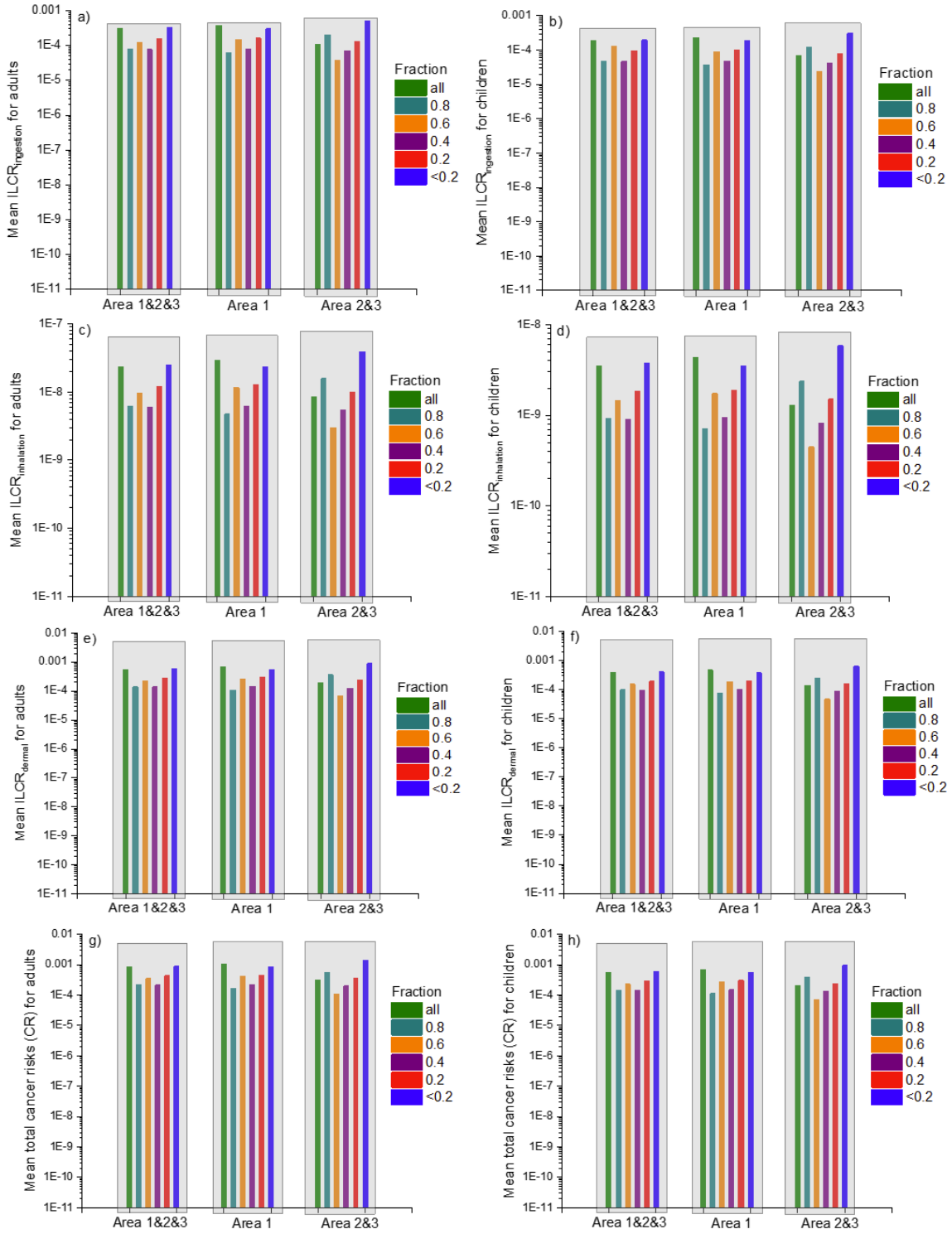

449

450 Figure 5. Mean concentrations of $\sum BaP_{TPE}$ of 16 PAH (CS) and results for incremental lifetime

451 cancer risk (ILCR) arising from PAH for adults (a,c,e) and children (b,d,f) received through each of

452 the main three pathways: ingestion ($ILCR_{ing}$) (a,b), inhalation ($ILCR_{inh}$) (c,d), and dermal contact

453 ($ILCR_{derm}$) (e,f), and total cancer risks (CR) (g, h) for street dust of Warsaw. ILCRs were calculated
454 for fractions "all", "0.8", "0.6", "0.4", "0.2", and "<0.2". ILCRs were calculated collectively for Areas
455 1&2&3 and separately for Area 1 and Area 2&3.

456 **3.7. Spatial distribution of $\sum PAH_{16}$ for fraction "<0.2"**

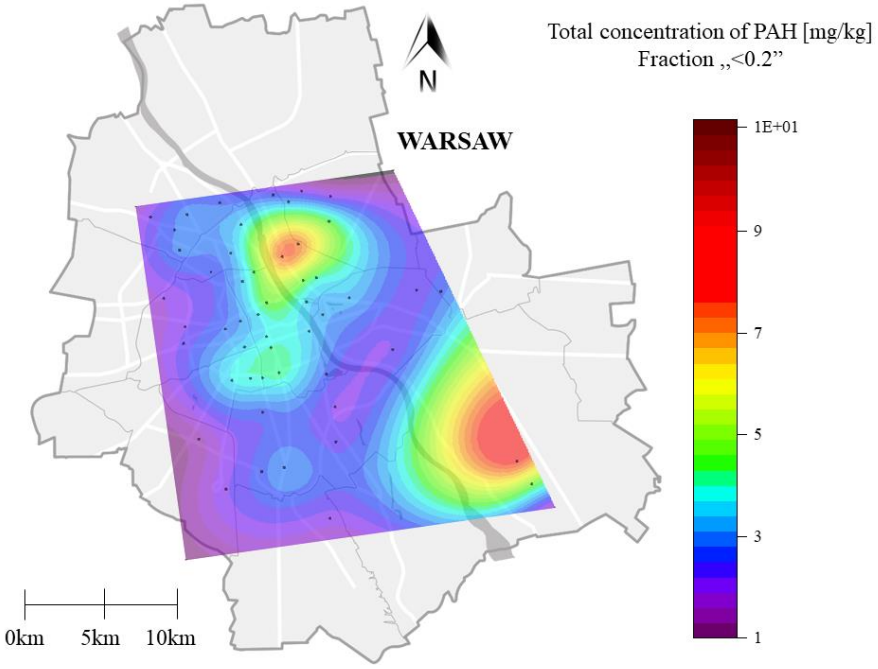

457

458 Figure 6. Spatial distribution of the interpolated mean $\sum PAH_{16}$ for fraction "<0.2" of 51 street dust
459 samples.

460 As shown in section 3.1., the most enriched in PAH (min. 1.0 ; max. 11.1 mg/kg; mean 3.4 mg/kg) is
461 the finest street dust fraction with grains with a diameter of less than 0.2 mm (200 um). This result
462 agreed with the PAH grain size distribution patterns reported in the previous studies (Lau and
463 Stenstrom, 2005; Lee et al., 2005). For road dust from Shenzhen (China) (Ning et al., 2019), it was
464 observed that mean $\sum PAH_{16}$ values attached to < 150 μm particles (~0.036 mg/kg) were higher than
465 those on > 150 μm.

466 The possible explanation for this effect might be that dominating PAH sources (traffic-related exhaust
467 and non-exhaust emissions, low-stack emission) produce fine particles (Rogge et al., 1993), whereas
468 coarse particles in street dust are mostly quartz sand, which does not carry high concentrations of PAH
469 (Murakami et al., 2005). Additionally, the finest fractions have a higher ability to accumulate PAH

because of the higher content of organic carbon and clay minerals and the larger surface area relative to their mass available for accumulation than the coarser one (Cornelissen et al., 2005).

Due to the highest PAH enrichment, the highest toxicity, and the highest health carcinogenic risk (see sections 3.4, 3.5, 3.6), a more detailed description was required, and the areal distribution is shown in Figure 6. Among samples containing the <0.2mm grains, the maximum $\sum PAH_{16}$ values occur on the right bank of the Vistula River and represent both Area 1 and Area 2&3. $\sum PAH_{16}$ values for the left bank of the Vistula River (Area 1) were in the range of 1 to 6 mg/g. The maximum values were observed at the sampling point from the city center for roads with high and medium traffic intensity and relatively low vehicle speed (speed restrictions up to 50 km/h). The two hotspots of total $\sum PAH_{16}$ values (9.08 and 11.09 mg/kg) are located in the NE part of Area 1 and the third maximum value (9.91 mg/kg) of $\sum PAH_{16}$ for fraction "<0.2" was obtained for the sampling site in SE part of Area 3. The three sampling sites with the lowest values of $\sum PAH_{16}$ (1.05, 1.1, and 1.74 mg/kg) were obtained for Area 1. The maximum $\sum PAH_{16}$ values are associated with streets with medium traffic intensity (from ~14,000 to 18,000 vehicles/day) and relatively compact architectural development at the very edge of the road. Two of the maximum sites are located relatively close to each other (1.2 km), whereas the sampling sites with $\sum PAH_{16}$ minimum values located in Area 1 are relatively close (2-3 km) to the $\sum PAH_{16}$ maximum sites. This can be explained by completely different types of land use that change over a short distance. Points with minimum values are located on roads with heavy and medium traffic, but at the same time next to a cemetery, green areas, and/or relatively sparse development of low buildings away from the edge of the road. The above factors significantly impact the distribution/transport of dust, especially in the case of small fractions, and thus on the final concentration of polluting factors contained in street dust. The minimum ∑PAH value for Area 2 (1.78 mg/kg) was obtained for single-lane roads with very low traffic intensity of <5,000 veh./day. However, other low ∑PAH concentrations (<2 mg/kg) in the SW study area (Area 1) were obtained for sampling sites located with high (10,000-20,000 veh/day) and/or very high (>20,000 veh/day) traffic intensity. Dong and Lee (2009) also found in areas without significant numbers of vehicle traffic, showing that other sources (low-stack emission) and/or pollution factors (e.g., vehicle speed, canyon road conditions, type of road surface) can influence the presence of PAH in urban street dust.

4. Conclusion

This study is considered to be one of the first investigations of 16 polycyclic aromatic hydrocarbons (PAH) in terms of distribution among six different grain-size fractions of street dust in a well-urbanized European city - Warsaw (Poland). However, such extensive research on the baseline PAH concentrations, toxicity, and health risk assessment determined for 169 samples representing various granulometric fractions of road dust has yet to be conducted for Poland.

We show that the highest concentration of PAH was found in the fraction with the smallest grain diameter (""<0.2"""). This observation is independent of the sampling area and the type of emission dominant in these areas. Moreover, the average concentration of PAH in the ""0.2"" fraction is significantly higher in Area 1 compared to Area 2&3. The difference is also significant in the ""0.6"" fraction. In general, the average PAH content in samples from Area 1 (central districts) was approximately 4 times higher than in samples from Area 2&3 (peripheral districts). The content of individual PAH was also different between these areas, so different chemical compounds dominate in samples from Area 1 and different ones in samples from Area 2&3.

The BaP_{TPE} was lower than in other studies, but the sum of carcinogenic PAH (CPAH) slightly exceeded the clean-up limit proposed by the Department of Ecology, State of Washington (2007). Our results indicate that the total ILCR values for adults and children exceeded the safe value significantly, reaching 10^{-3}, indicating a high potential carcinogenic risk. Furthermore, much higher CR values ($>10^{-4}$) than for other granulometric fractions were found for both children and adults in the fraction "<0.2". Hence, scientific and governmental attention should be paid to the PAH pollution of street dust in Warsaw because of the PAH' high potential carcinogenic risk for residents.

The spatial distribution of $\sum PAH_{16}$ concentrations for the "<0.2" fraction, taking into account land use, showed the following pattern: high-density architecture, multi-lane roads > residential, city center, low buildings > green areas, sparse type of architecture.

This study contributed to filling the gap in knowledge about the characteristics of PAH contaminants in the subject of the grain size of street dust from Warsaw and assessing the potential health risks of people exposed to PAH contaminants. Therefore, our work has provided new significant information

525 on PAH pollution, methods of measuring PAH' content, and assessing the risk to human health, which
526 may be useful to the scientific community, policymakers, and the general public.

527 **3. References**

528 Abbasi, S., Keshavarzi, B., 2019. Source identification of total petroleum hydrocarbons and polycyclic
529 aromatic hydrocarbons in PM10 and street dust of a hot spot for petrochemical production: Asaluyeh
530 County, Iran. Sustain. Cities Soc., 45, 214-230. https://doi.org/10.1016/j.scs.2018.11.015.

531 Adeel, M., Song, X., Wang, Y., Francis, D., Yang, Y., 2017. Environmental impact of estrogens on
532 human, animal and plant life: a critical review. Environ. Int., 99, 107–119.
533 https://doi.org/10.1016/j.envint.201 http://aphekom.org/web/aphekom.org/home6.12.010.

534 Aphekom, 2011. Aphekom project. http://aphekom.org/web/aphekom.org/home [accessed July 2024]

535 Cao, Z., Zhao, L., Shi, Y., Feng, J., Wang, S., Zhang, Y., Yan, G., Zhang, X., Wang, X., Shen, M.,
536 Wang, Y., 2017. PAH contamination in road dust from a moderate city in North China: the significant
537 role of traffic emission. Hum. Ecol. Risk Assess. 23, 1072–1085.
538 https://doi.org/10.1080/10807039.2017.1300768.

539 Chen, M., Huang, P., Chen, L., 2013. Polycyclic aromatic hydrocarbons in soils from Urumqi,
540 Environ. Monit. Assess., 185, 5639–5651. https://doi.org/10.1007/s10661-012-2973-6.

541 Cornelissen, G., Gustafsson, O., Bucheli, T.D., Jonker, M.T.O., Koelmans, A.A., Van Noort, P.C.M.,
542 2005. Extensive sorption of organic compounds to black carbon, coal, and kerogen in sediments and
543 soils: mechanisms and consequences for distribution, bioaccumulation, and biodegradation. Environ.
544 Sci. Technol., 39, 6881–6895. https://doi.org/10.1021/es050191b.

545 Davoudi, M., Esmaili-Sari, A., Bahramifar, N., Moeinaddini, M., 2021.Spatio-temporal variation and
546 risk assessment of polycyclic aromatic hydrocarbons (PAH) in surface dust of Qom metropolis, Iran.
547 Environ. Sci. Pollut. Res., 28, 9276–9289. https://doi.org/10.1007/s11356-020-08863-5.

548 Deletic, A., Orr, D. W., 2005. Pollution buildup on road surfaces. J. Environ. Eng., 131(1), 49–59.
549 https://doi.org/10.1061/(ASCE)0733-9372(2005)131:1(49).

550 Department of Ecology, State of Washington, 2007. Evaluating the toxicity and assessing
551 the carcinogenic risk of environmental mixtures using toxicity equivalency factors.
552 available at: https://fortress.wa.gov/ecy/clarc/FocusSheets/tef.pdf. [ccessed June 2024]

Dong, T.T., Lee, B.K., 2009. Characteristics, toxicity, and source apportionment of polycylic aromatic hydrocarbons (PAH) in road dust of Ulsan, Korea. Chemosphere, 74 (9), 1245–1253. https://doi.org/10.1016/j.chemosphere.2008.11.035.

Dytłow S., Winkler A., Górka-Kostrubiec B., Sagnotti L., 2019. Magnetic, geochemical and granulometric properties of street dust from Warsaw (Poland). J. Appl. Geophys., 169, 58–73. https://doi.org/10.1016/j.jappgeo.2019.06.016.

Franco, C.F.J., de Resende, M.F., de Almeida Furtado, L., Figueredo Brasil, T., Eberlin, M.N., Pereira Netto, A.D., 2017. Polycyclic aromatic hydrocarbons (PAH) in street dust of Rio de Janeiro and Niterói, Brazil: Particle size distribution, sources and cancer risk assessment. Sci. Total Environ., 599–600, 305-313, https://doi.org/10.1016/j.scitotenv.2017.04.060.

Gope, M., Masto, R.E., George, J., Balachandran, S., 2018. Exposure and cancer risk assessment of polycyclic aromatic hydrocarbons (PAH) in the street dust of Asansol city, India. Sustain. Cities Soc., 38, 616–626. https://doi.org/10.1016/j.scs.2018.01.006.

Gunawardana, C., Goonetilleke, A., Egodawatta, P., Dawes, L., Kokot, S. 2012. Role of Solids in Heavy Metals Buildup on Urban Road Surfaces. Environ. Eng. ASCE., 138,490–498. https://doi.org/10.1061/(ASCE)EE.1943-7870.0000487.

GUS, 2023. Powierzchnia i ludność w przekroju terytorialnym w 2023 roku, https://stat.gov.pl/obszary-tematyczne/ludnosc/ludnosc/powierzchnia-i-ludnosc-w-przekroju-terytorialnym-w-2023-roku,7,20.html [accessed July 2024].

Ha, S.Y., Kim, G.B., Yim, U.H., Shim, W.J., Hong, S.H., Han, G.M., 2012. Particle-Size Distribution of Polycyclic Aromatic Hydrocarbons in Urban Road Dust of Masan, Korea. Arch. Environ. Contam. Toxicol., 63, 189–198. https://doi.org/10.1007/s00244-012-9765-4.

Haynes, H.M., Taylor, K.G., Rothwell, J., Byrne, P., 2020. Characterisation of road-dust sediment in urban systems: A review of a global challenge. J. Soils Sedim., 20, 4194–4217. https://doi.org/10.1007/s11368-020-02804-y.

Hussain, K., Rahman, M., Prakash, A., Hoque, R.R., 2015. Street dust bound PAH, carbon and heavy metals in Guwahati city–Seasonality, toxicity and sources. Sustain Cities Soc., 19, 17–25. https://doi.org/10.1016/j.scs.2015.07.010.

IARC, 1987. Overall evaluations of carcinogenicity: An updating of IARC monographs volumes 1 to 42, IARC monographs on the evaluation of carcinogenic risks to humans, supplement 7. Lyon: International Agency for Research on Cancer.

Kamal, A., Malik, R.N., Martellini, T., Cincinelli, A., 2015. Source, profile, and carcinogenic risk assessment for cohorts occupationally exposed to dust-bound PAH in Lahore and Rawalpindi cities (Punjab province, Pakistan). Environ. Sci. Pollut. Res. Int., 22(14), 10580–10591. https://doi.org/10.1007/s11356-015-4215-2.

Kamal, A., Malik, R.N., Martellini, T., Cincinelli, A., 2014. Cancer risk evaluation of brick kiln workers exposed to dust bound PAH in Punjab province (Pakistan). Sci. Total Environ., 493, 562-570. https://doi.org/10.1016/j.scitotenv.2014.05.140.

Kaneda, T., Greenbaum, C., Patierno, K., 2015. World population data sheet. Washington: Population Reference Bureau. https://interactives.prb.org/2021-wpds/ [Accessed July 2024].

Kannan, K., Johnson-Restrepo, B., Yohn, S.S., Giesy, J.P., Long, D.T., 2005. Spatial and temporal distribution of polycyclic aromatic hydrocarbons in sediments from Michigan inland lakes. Environ. Sci. Technol., 39(13), 4700–4706. https://doi.org/10.1021/es050064f.

Kreider, M.L., Panko, J.M., McAtee, B.L., Sweet, L.I., Finley, B.L., 2010. Physical and chemical characterization of tire-related particles: Comparison of particles generated using different methodologies. Sci. Total Environ., 408, 652–659. https://doi.org/10.1016/j.scitotenv.2009.10.016.

Larsen, R.K., Baker, J.E., 2003. Source apportionment of polycyclic aromatic hydrocarbons in the urban atmosphere: a comparison of three methods. Environ. Sci. Technol., 37(9),1873–1881. https://doi.org/10.1021/es0206184.

Lau, S.-L., Stenstrom, M.K., 2005. Metals and PAH adsorbed to street particles. Water Res. 39, 4083–4092. https://doi.org/10.1016/j.watres.2005.08.002.

Lee, B.-C., Shimizu, Y., Matsuda, T., Matsui, S., 2005. Characterization of polycyclic aromatic hydrocarbons (PAH) in different size fractions in deposited road particles (DRPs) from Lake Biwa area, Japan. Environ. Sci. Technol., 39, 7402–7409. https://doi.org/10.1021/es050103n.

Li, Z., Feng, X., Li, G., Bi, X., Zhu, J., Qin, H., Dai, Z., Liu, J., Li, Q., Sun, G., 2013. Distributions, sources and pollution status of 17 trace metal/metalloids in the street dust of a heavily industrialized city of central China. Environ. Pollut., 182, 408–416. https://doi.org/10.1016/j.envpol.2013.07.041.

Logiewa, A., Miazgowicz, A., Krennhuber, K., Lanzerstorfer, C., 2020. Variation in the concentration of metals in road dust size fractions between 2 μm and 2 mm: results from three metallurgical centres in Poland. Arch. Environ. Contam. Toxicol. 78 (1), 46–59. https://doi.org/10.1007/s00244-019-00686-x.

Lorenzi, D., Entwistle, J.A., Cave, M., Dean, J.R., 2011. Determination of polycyclic aromatic hydrocarbons in urban street dust: implications for human health. Chemosphere 83, 970–977. https://doi.org/10.1016/j.chemosphere.2011.02.020.

Ma, Y., Harrad, S., 2015. Spatiotemporal analysis and human exposure assessment on polycyclic aromatic hydrocarbons in indoor air, settled house dust, and diet: a review. Environ. Intl. 84, 7–16. https://doi.org/10.1016/j.envint.2015.07.006.

Mansouri, E., Yousefi, V., Ebrahimi, V., Eyvazi, S., Saeid Hejazi, M., Mahdavi, M., Mesbahi, A., Tarhriz, V., 2020. Overview of ultraviolet-based methods used in polycyclic aromatic hydrocarbons analysis and measurement. Sep. Sci. plus 3, 112–120. https://doi.org/10.1002/sscp.201900077.

Murakami, M., Nakajima, F., Furumai, H., 2005. Size- and density-distributions and sources of polycyclic aromatic hydrocarbons in urban road dust. Chemosphere 61, 783–791. https://doi.org/10.1016/j.chemosphere.2005.04.003.

Ning, Y., Guo, Z., Zhang, J., Niu, S., He, B., Xiao, K., Liu, A., 2023. Characterizing polycyclic aromatic hydrocarbons on road dusts in Shenzhen, China: implications for road stormwater reuse safety. Environ. Geochem. Health , 45, 4951–4963. https://doi.org/10.1007/s10653-023-01547-2.

Nisbet, I.C.T., LaGoy, P.K., 1992. Toxic equivalency factors (TEFs) for polycyclic aromatic hydrocarbons (PAH). Regul. Toxicol. Pharmacol., 16 (3),290–300. https://doi.org/ 10.1016/0273-2300(92)90009-X Academic Press.

Pathak, A.K., Yadav, S., Kumar, P., Kumar, R., 2013. Source apportionment and spatial-temporal variations in the metal content of surface dust collected from an industrial area adjoining Delhi, India. Sci. Total Environ., 443, 662-672. https://doi.org/10.1016/j.scitotenv.2012.11.030.

635 Peng, C., Chen, W.P., Liao, X.L., Wang, M.E., Ouyang, Z.Y., Jiao, W.T., 2011. Polycyclic aromatic
636 hydrocarbons in urban soils of Beijing: Status, sources, distribution and potential risk. Environ.
637 Pollut., 15, 802–808. https://doi.org/10.1016/j.envpol.2010.11.003.
638 Puy-Alquiza, M.J., Reyes, V., Wrobel, K., Wrobel, K., Torres Elguera, J.C., Miranda-Aviles, R., 2016.
639 Polycyclic aromatic hydrocarbons in urban tunnels of Guanajuato city (Mexico) measured in deposited
640 dust particles and in transplanted lichen Xanthoparmelia mexicana (Gyeln.) Hale. Environ Sci. Pollut.
641 Res., 23, 11947–11956. https://doi.org/10.1007/s11356-016-6256-6.
642 Rogge, W.F., Hidemann, L.M., Mazurek, M.A., Cass, G.R., 1993. Sources of fine organic aerosol. 3.
643 Road dust, tire debris, and organometallic brake lining dust: Roads as sources and sinks. Environ. Sci.
644 Technol., 27, 1892–1904. https://doi.org/10.1021/es00046a019.
645 Sarigiannis, D.A., Karakitsios, S.P., Zikopoulos, D., Nikolaki, S., Kermenidou, M., 2015. Lung cancer
646 risk from PAH emitted from biomass combustion. Environ. Res., 137, 147–156.
647 https://doi.org/10.1016/j.envres.2014.12.009.
648 Skrbic, B. Durisic-Mladenovic, N., Zivancev, J., Tadic, D., 2019. Seasonal occurrence and cancer risk
649 assessment of polycyclic aromatic hydrocarbons in street dust from the Novi Sad city, Serbia. Sci.
650 Total Environ., 647, 191-203. https://doi.org/10.1016/j.scitotenv.2018.07.442.
651 Soltani, N., Keshavarzi, B., Moore, F., Tavakol, T., Lahijanzadeh, A.R., Jaafarzadeh, N., Kermani, M.,
652 2015. Ecological and human health hazards of heavy metals and polycyclic aromatic hydrocarbons
653 (PAH) in road dust of Isfahan metropolis, Iran. Sci. Total Environ. 505, 712–723.
654 https://doi.org/10.1016/j.scitotenv.2014.09.097.
655 Tanner, P. A., Ma, H., Yu, A.K.N., 2008. Fingerprinting metals in urban street dust of Beijing,
656 Shanghai, and Hong Kong. Environ. Sci. Technol., 42, 7111–7117. https://doi.org/10.1021/es8007613.
657 Tobiszewski, M., Namiesnik, J., 2012. PAH diagnostic ratios for the identification of pollution
658 emission sources. Environ. Pollut., 162, 110–119. https://doi.org/10.1016/j.envpol.2011.10.025.
659 Gennadiev, A.N., Tsibart, A.S., 2013. Pyrogenic polycyclic aromatic hydrocarbons in soils of reserved
660 and anthropogenically modified areas: Factors and features of accumulation. Eurasian Soil Sc., 46, 28–
661 36. https://doi.org/10.1134/S106422931301002X

UN, 2019. World urbanization prospects the 2018 revision. UN, New York. https://population.un.org/wup/Publications/Files/WUP2018-Report.pdf [accessed July 2024].

UNDESA 2018. World urbanization prospects: the 2018 revision. https://population.un.org/wup/Publications/Files/WUP2018-Report.pdf. [Accessed July 2024].

USEPA, 2011. U.S. Environmental Protection Agency, 2011. Exposure Factors Handbook. 2011 ed., Final Report. Environmental Protection Agency, Washington, DC EPA/600/R-09/052F.

USEPA, 2014. U.S. Environmental Protection Agency, 2014. Human health evaluation manual, supplemental guidance: update of standard default exposure factors. OSWER Directive 9200 1–120.

Wang, W., Huang, M., Kang, Y., Wang, H., Leung, A. O. W., Cheung, K. C., et al., 2011. Polycyclic aromatic hydrocarbons (PAH) in urban surface dust of Guangzhou, China: Status, sources and human health risk assessment. Sci.Total Environ., 409, 4519–4527. https://doi.org/10.1016/j.scitotenv.2011.07.030.

Wang, C., Wu, S., Zhou, S.L., Wang, H., Li, B., Chen, H., Yu, Y., Shi, Y., 2015. Polycyclic aromatic hydrocarbons in soils from urban to rural areas in Nanjing: concentration, source, spatial distribution, and potential human health risk. Sci. Total Environ., 527–528, 375–383. https://doi.org/10.1016/j.scitotenv.2015.05.025.

WBR, 2023. Warszawskie badanie Ruchu. https://zdm-warszawa.maps.arcgis.com/apps/dashboards/9482f44e811f472a8e9a68405eb86517. [Accessed July 2024].

WHO, 2016. World Health Organization; Geneve, Switzerland. Ambient Air Pollution: A Global Assessment of Exposure and Burden of Disease. p. 121.

Yang, T., Liu, Q., Li, X., Zeng, Q., Chan, L., 2010. Anthropogenic magnetic particles and heavy metals in the road dust: Magnetic identification and its implications. Atmospheric Environment, 44, 1175–1185. https://doi.org/10.1016/j.atmosenv.2009.12.028.

Yildirim, G., Tokalioğlu, Ş., 2016. Heavy metal speciation in various grain sizes of industrially contaminated street dust using multivariate statistical analysis. Ecotoxicol. Environ. Saf., 369–376. https://doi.org/10.1016/j.ecoenv.2015.11.006.

Yusuf, R.O., Odediran, E.T., Adeniran, J.A., Adesina, O.A., 2022. Polycyclic aromatic hydrocarbons in road dusts of a densely populated African city: spatial and seasonal distribution, source, and risk assessment. Environ. Sci. Pollut. Res., 29, 44970–44985. https://doi.org/10.1007/s11356-022-18943-3.

Acknowledgments

This research was funded in whole by the National Science Centre (Poland), grant number 2021/43/D/ST10/00996. For the purpose of Open Access, the author has applied a CC-BY public copyright licence to any Author Accepted Manuscript (AAM) version arising from this submission. This work was supported by a subsidy from the Polish Ministry of Education and Science for the Institute of Geophysics, Polish Academy of Sciences. The authors would like to thank Dominika Kwiecień, a student who participated in the field and laboratory work but did not contribute to the content of the publication. We thank Klaudia Tetfejer for contributing her technical expertise and for assisting with data collection.

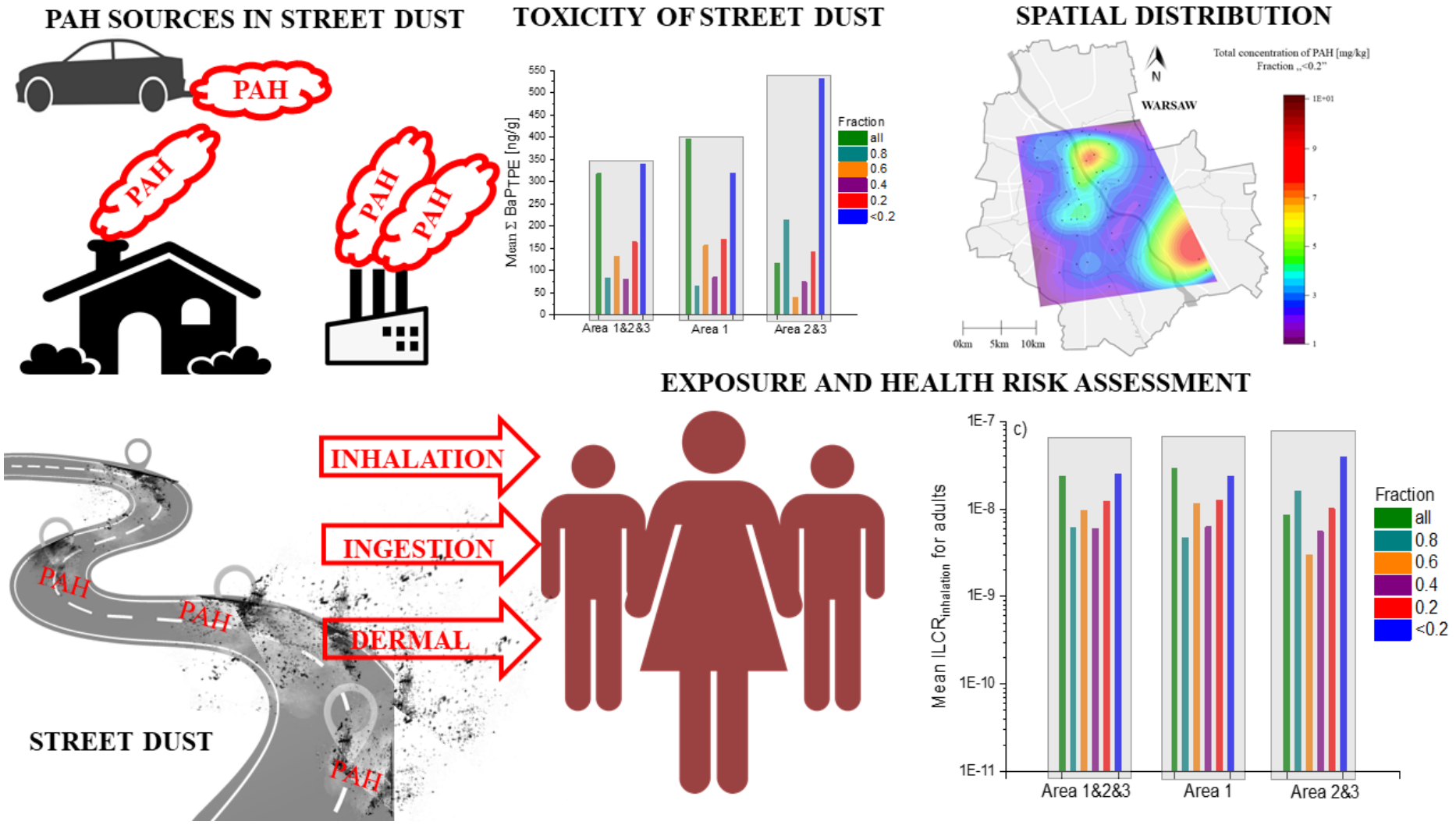
PAH SOURCES IN STREET DUST
PAH
PAH
PAH
PAH
TOXICITY OF STREET DUST
Mean Σ BaPTPE [ng/g]
550
500
450
400
350
300
250
200
150
100
50
0
Area 1&2&3
Area 1
Area 2&3
Fraction
all
0.8
0.6
0.4
0.2
<0.2
SPATIAL DISTRIBUTION
N
WARSAW
Total concentration of PAH [mg/kg]
Fraction „<0.2"
1E+01
9
7
5
3
1
0km
5km
10km
EXPOSURE AND HEALTH RISK ASSESSMENT
INHALATION
INGESTION
DERMAL
PAH
PAH
PAH
STREET DUST
c)
Mean ILCR inhalation for adults
1E-7
1E-8
1E-9
1E-10
1E-11
Area 1&2&3
Area 1
Area 2&3
Fraction
all
0.8
0.6
0.4
0.2
<0.2

Supplementary materials

Basic separation and detection parameters	
Instrument	HPLC Agilent 1290 with 1260 DAD
Elution	Gradient: 0.0 min 70% A 9.0 min 0% A 14.0 min 0% A 14.1 min 70% A 17.0 min 70% A
Flow rate	0.35 ml/min
Injection volume	5 µL
Column	Phenomenex Kinetex 3.5 µm PAH, 100*2.1 mm @ 40ºC
Detection	254.0 nm, Ref = 400.0 nm

Table S1 Chromatographic and detection parameters used in the determination of PAH.

Parameter	Description	Unit	Adults	Children	References
ABS	Dermal-Absorption-Factor	unitless	0.13	0.13	(US EPA, 2011)
BW	Body-Weight	Kg	70	15	(US EPA, 2014)
ED	Exposure-Duration	Years	20	6	(US EPA, 2014)
AF	Dermal-Adherence-Factor	mg/cm^2	0.07	0.2	(US EPA, 2011)
AT	Average-Time (70years_365 days/year)	Days	25,550	25,550	(Soltani et al., 2015)
IR ingestion	Ingestion-Rate	mg/day	100	200	(US EPA, 2011)
IR inhalation	Inhalation-Rate	m^3/day	20	10	(Soltani et al., 2015)
EF	Exposure-Frequency	days/year	350	350	(US EPA, 2014)
PEF	Particular-Emission-Factor	m^3/kg	1.36×10^{9}	1.36×10^{9}	(US EPA, 2014)
SA	Dermal-Surface-Area-Exposure	cm^2	5700	2800	(US EPA, 2014)

Table S2 The parameters used for incremental life cancerogenic risk (ILCR) calculations.

		Parameter for $\sum BaP_{TPE}$ [ng/g]			
Fraction	Area	Minimum	Maximum	Mean	Standard Deviation
<0.2	1&2&3	33.9	1418.1	339.7	241.3
<0.2	1	33.9	1298.5	318.9	192.5
<0.2	2&3	208.2	1418.1	531.6	509.5
0.2	1&2&3	0.4	554.8	164.3	160.6
0.2	1	11.8	554.8	170.5	163.8
0.2	2&3	0.4	398.6	143.3	165.4
0.4	1&2&3	0.0	283.9	81.4	98.4
0.4	1	0.0	270.4	84.5	92.1
0.4	2&3	0.0	283.9	74.6	122.6
0.6	1&2&3	0.0	593.1	131.7	150.2
0.6	1	0.0	593.1	157.0	159.6
0.6	2&3	0.0	95.8	40.5	50.4
0.8	1&2&3	0.0	870.1	83.4	159.1
0.8	1	0.0	344.6	64.1	97.4
0.8	2&3	0.0	870.1	214.6	370.9
all	1&2&3	3.4	1168.2	318.3	303.2
all	1	110.0	1168.2	395.9	316.9
all	2&3	3.4	337.6	116.5	137.0

Table S3 Statistical description of $\sum BaP_{TPE}$ for samples “all” and granulometric fractions of street dust.

	Ingestion		Inhalation		Dermal		Parameter	Area	Fraction
CS[ng/g]	Adult	Child	Adult	Child	Adult	Child			
3.39E+01	3.23E-05	1.94E-05	2.50E-09	3.75E-10	5.73E-05	4.02E-05	Min.	1&2&3	<0.2
1.42E+03	1.35E-03	8.10E-04	1.05E-07	1.57E-08	2.40E-03	1.68E-03	Max.		
3.40E+02	3.24E-04	1.94E-04	2.51E-08	3.76E-09	5.75E-04	4.03E-04	Mean		
1.30E+03	3.23E-05	1.94E-05	2.50E-09	3.75E-10	5.73E-05	4.02E-05	Min.	1	
1.30E+03	1.24E-03	7.42E-04	9.59E-08	1.44E-08	2.20E-03	1.54E-03	Max.		
3.40E+02	3.04E-04	1.82E-04	2.36E-08	3.53E-09	5.39E-04	3.79E-04	Mean		
2.08E+02	1.98E-04	1.19E-04	1.54E-08	2.31E-09	3.52E-04	2.47E-04	Min.	2&3	
1.42E+03	1.35E-03	8.10E-04	1.05E-07	1.57E-08	2.40E-03	1.68E-03	Max.		
5.32E+02	5.06E-04	3.04E-04	3.93E-08	5.89E-09	8.99E-04	6.31E-04	Mean		
4.05E-01	3.86E-07	2.31E-07	2.99E-11	4.49E-12	6.85E-07	4.81E-07	Min.	1&2&3	0.2
5.55E+02	5.28E-04	3.17E-04	4.10E-08	6.15E-09	9.39E-04	6.59E-04	Max.		
1.64E+02	1.57E-04	9.39E-05	1.21E-08	1.82E-09	2.78E-04	1.95E-04	Mean		
1.18E+01	1.13E-05	6.77E-06	8.75E-10	1.31E-10	2.00E-05	1.41E-05	Min.	1	
5.55E+02	5.28E-04	3.17E-04	4.10E-08	6.15E-09	9.39E-04	6.59E-04	Max.		
1.71E+02	1.62E-04	9.74E-05	1.26E-08	1.89E-09	2.88E-04	2.02E-04	Mean		
4.05E-01	3.86E-07	2.31E-07	2.99E-11	4.49E-12	6.85E-07	4.81E-07	Min.	2&3	
3.99E+02	3.80E-04	2.28E-04	2.94E-08	4.42E-09	6.74E-04	4.73E-04	Max.		
1.43E+02	1.30E-04	7.80E-05	1.01E-08	1.51E-09	2.31E-04	1.62E-04	Mean		
0.00E+00	0.00E+00	0.00E+00	0.00E+00	0.00E+00	0.00E+00	0.00E+00	Min.	1&2&3	0.4
2.84E+02	2.70E-04	1.62E-04	2.10E-08	3.15E-09	4.80E-04	3.37E-04	Max.		
8.14E+01	7.76E-05	4.65E-05	6.02E-09	9.02E-10	1.38E-04	9.67E-05	Mean		
0.00E+00	0.00E+00	0.00E+00	0.00E+00	0.00E+00	0.00E+00	0.00E+00	Min.	1	
2.70E+02	2.58E-04	1.55E-04	2.00E-08	3.00E-09	4.57E-04	3.21E-04	Max.		
8.45E+01	8.05E-05	4.83E-05	6.25E-09	9.37E-10	1.43E-04	1.00E-04	Mean		
0.00E+00	0.00E+00	0.00E+00	0.00E+00	0.00E+00	0.00E+00	0.00E+00	Min.	2&3	
2.84E+02	2.70E-04	1.62E-04	2.10E-08	3.15E-09	4.80E-04	3.37E-04	Max.		
7.46E+01	7.11E-05	4.26E-05	5.51E-09	8.27E-10	1.26E-04	8.86E-05	Mean		
0.00E+00	0.00E+00	0.00E+00	0.00E+00	0.00E+00	0.00E+00	0.00E+00	Min.	1&2&3	0.6
5.93E+02	5.65E-04	3.39E-04	4.38E-08	6.57E-09	1.00E-03	7.04E-04	Max.		
1.33E+02	1.25E-04	7.52E-05	9.73E-09	1.46E-09	2.23E-04	1.56E-04	Mean		
0.00E+00	0.00E+00	0.00E+00	0.00E+00	0.00E+00	0.00E+00	0.00E+00	Min.	1	
5.93E+02	5.65E-04	3.39E-04	4.38E-08	6.57E-09	1.00E-03	7.04E-04	Max.		
1.57E+02	1.50E-04	8.97E-05	1.16E-08	1.74E-09	2.66E-04	1.86E-04	Mean		
0.00E+00	0.00E+00	0.00E+00	0.00E+00	0.00E+00	0.00E+00	0.00E+00	Min.	2&3	
9.58E+01	9.12E-05	5.47E-05	7.08E-09	1.06E-09	1.62E-04	1.14E-04	Max.		
4.05E+01	3.86E-05	2.32E-05	2.99E-09	4.49E-10	6.86E-05	4.81E-05	Mean		
0.00E+00	0.00E+00	0.00E+00	0.00E+00	0.00E+00	0.00E+00	0.00E+00	Min.	1&2&3	0.8
8.70E+02	8.29E-04	4.97E-04	6.43E-08	9.64E-09	1.47E-03	1.03E-03	Max.		
8.34E+01	7.94E-05	4.76E-05	6.16E-09	9.24E-10	1.41E-04	9.90E-05	Mean		
0.00E+00	0.00E+00	0.00E+00	0.00E+00	0.00E+00	0.00E+00	0.00E+00	Min.	1	
3.45E+02	3.28E-04	1.97E-04	2.55E-08	3.82E-09	5.83E-04	4.09E-04	Max.		
6.41E+01	6.10E-05	3.66E-05	4.73E-09	7.10E-10	1.08E-04	7.61E-05	Mean		
0.00E+00	0.00E+00	0.00E+00	0.00E+00	0.00E+00	0.00E+00	0.00E+00	Min.	2&3	
8.70E+02	8.29E-04	4.97E-04	6.43E-08	9.64E-09	1.47E-03	1.03E-03	Max.		
2.15E+02	2.04E-04	1.23E-04	1.59E-08	2.38E-09	3.63E-04	2.55E-04	Mean		
3.38E+00	3.22E-06	1.93E-06	2.50E-10	3.74E-11	5.72E-06	4.01E-06	Min.	1&2&3	all
1.17E+03	1.11E-03	6.68E-04	8.63E-08	1.29E-08	1.98E-03	1.39E-03	Max.		
3.18E+02	3.03E-04	1.82E-04	2.35E-08	3.53E-09	5.39E-04	3.78E-04	Mean		
1.10E+02	1.05E-04	6.28E-05	8.12E-09	1.22E-09	1.86E-04	1.31E-04	Min.	1	
1.17E+03	1.11E-03	6.68E-04	8.63E-08	1.29E-08	1.98E-03	1.39E-03	Max.		
3.96E+02	3.77E-04	2.26E-04	2.92E-08	4.39E-09	6.70E-04	4.70E-04	Mean		
3.38E+00	3.22E-06	1.93E-06	2.50E-10	3.74E-11	5.72E-06	4.01E-06	Min.	2&3	
3.38E+02	3.22E-04	1.93E-04	2.49E-08	3.74E-09	5.71E-04	4.01E-04	Max.		
1.16E+02	1.11E-04	6.66E-05	8.60E-09	1.29E-09	1.97E-04	1.38E-04	Mean		

Table S4 Concentrations of $\sum BaP_{TPE}$ of 16 PAH (CS) and results for incremental lifetime cancer risk (ILCR) of a PAH received through each of the main three pathways: ingestion, inhalation, and dermal contact. ILCRs were calculated for fractions “all”, “0.8”, “0.6”, “0.4”, “0.2”, and “<0.2”. ILCRs were calculated collectively for Areas 1&2&3 and separately for Area 1 and Area 2&3.